

## Tests of the Standard Model in Leptonic Reactions at PETRA Energies

JADE Collaboration

W. Bartel, L. Becker, D. Cords<sup>1</sup>, R. Felst, D. Haidt, G. Knies, H. Krehbiel, P. Laurikainen<sup>2</sup>,  
N. Magnussen<sup>3</sup>, R. Meinke, B. Naroska, J. Olsson, D. Schmidt<sup>3</sup>, P. Steffen

Deutsches Elektronen-Synchrotron DESY, D-2000 Hamburg, Federal Republic of Germany

G. Dietrich, J. Hagemann, G. Heinzlmann, H. Kado, K. Kawagoe<sup>4</sup>, C. Kleinwort, M. Kuhlen,  
A. Petersen<sup>1</sup>, R. Ramcke, U. Schneekloth, G. Weber

II. Institut für Experimentalphysik der Universität, D-2000 Hamburg, Federal Republic of Germany

K. Ambrus, S. Bethke, A. Dieckmann, E. Elsen, J. Heintze, K.H. Hellenbrand, S. Komamiya,  
J. von Krogh, P. Lennert, H. Matsumura, H. Rieseberg, J. Spitzer, A. Wagner

Physikalisches Institut der Universität, D-6900 Heidelberg, Federal Republic of Germany

C. Bowdery, A. Finch, F. Foster, G. Hughes, J. Nye

University of Lancaster, Lancaster LA1 4YB, England

J. Allison, A.H. Ball<sup>6</sup>, R.J. Barlow, J. Chrin, I.P. Duerdoth, T. Greenshaw, P. Hill, F.K. Loebinger,  
A.A. Macbeth, H.E. Mills, P.G. Murphy, K. Stephens, P. Warming

University of Manchester, Manchester M13 9PL, England

R.G. Glasser, J.A.J. Skard, S.R. Wagner<sup>5</sup>, G.T. Zorn

University of Maryland, College Park, MD 20742, USA

S.L. Cartwright, D. Clarke, R. Marshall, R.P. Middleton

Rutherford Appleton Laboratory, Chilton, Oxon OX11 0QX, England

T. Kawamoto, T. Kobayashi, H. Takeda, T. Takeshita, S. Yamada

International Center for Elementary Particle Physics, University of Tokyo, Japan

Received 29 November 1985

**Abstract.** An analysis of the three leptonic reactions  $e^+e^- \rightarrow e^+e^-$ ,  $\mu^+\mu^-$  and  $\tau^+\tau^-$  over a wide range of energy,  $12 < \sqrt{s} < 46.78$  GeV is presented. The data were obtained with the JADE detector at the  $e^+e^-$  storage ring PETRA. They are compared to pre-

dictions of electroweak theories, in particular the standard model. For the total cross-sections of all three reactions and for the differential cross-section of Bhabha scattering no deviation from QED is found over the entire energy range. The differential cross-sections of  $\mu$  and  $\tau$  pairs at high energies show the angular asymmetry predicted by electroweak interference. The axial-vector and vector weak coupling constants,  $\sin^2\theta_w$  and  $M_Z$  are determined and compared to other measurements. Finally, limits on deviations from the standard model are given.

<sup>1</sup> Now at SLAC, California, USA

<sup>2</sup> University of Helsinki, Helsinki, Finland

<sup>3</sup> Universität-Gesamthochschule Wuppertal, FRG

<sup>4</sup> DAAD fellow

<sup>5</sup> Now at University of Colorado

<sup>6</sup> Now at University of Maryland

## Introduction

In the period 1980–1984 the JADE detector at PETRA was used to collect data on the production of lepton pairs,  $e^+e^- \rightarrow e^+e^-$ ,  $\mu^+\mu^-$  and  $\tau^+\tau^-$ . These data were used to test predictions of electroweak theories, specifically the standard model of Glashow et al. [1]. The main deviation from QED predicted by electroweak theories, which is measurable at  $e^+e^-$  storage rings with energies well below the mass of the  $Z^0$ , is an angular asymmetry for muon- and tau-pairs. This is an effect of the interference of the two neutral currents contributing, the electromagnetic and the weak neutral current. The total event rate on the other hand is not expected to be affected measurably by electroweak effects. In Bhabha scattering which is dominated by  $t$ -channel exchange the electroweak interference effects on the angular distribution are less pronounced than for muon and tau production.

The weak axial-vector and vector coupling constants are determined by comparing the data with the theoretical predictions. These comparisons can be made for the three processes separately and thus universality between electrons, muons and taus which is a fundamental assumption of the standard model is tested. This is of particular interest with regard to  $\tau$  pairs since their properties with respect to the weak neutral current are not well known and  $e^+e^-$  interactions provide so far the only possibility to study them. Furthermore constraints are obtained on the weak mixing angle  $\sin^2\theta_W$  and the mass  $M_Z$  of the weak intermediate boson  $Z^0$ . Finally limits on deviations from the standard theory which are allowed within the experimental errors are computed.

## The Data

The data were collected at center-of-mass energies  $12 \leq \sqrt{s} \leq 46.78$  GeV and correspond to a total integrated luminosity of  $103 \text{ pb}^{-1}$ . The data were partially taken in energy scans, where the beam energy was increased in fine steps; therefore the exact average value of  $s$  depends on how the data were binned. Approximately  $75 \text{ pb}^{-1}$  were taken at energies around  $\sqrt{s} = 34.5$  GeV and approximately  $27 \text{ pb}^{-1}$  around  $\sqrt{s} = 43.4$  GeV. The detector and the analysis procedures have been described in previous publications [2–4]. For the analyses presented in this paper, also data at the highest PETRA energies, which have not been published before, will be included.

The numerical values of the data used are summarized in Tables 4–7 at the end of the paper. The differential and total cross-sections for  $e^+e^- \rightarrow e^+e^-$ ,  $\mu^+\mu^-$  and  $\tau^+\tau^-$  at energies above  $\sqrt{s} \sim 30$  GeV are also shown in Figs. 1–4. The data are corrected for detection efficiencies as well as for higher order QED effects. QED diagrams up to order  $\alpha^3$  were included in the corrections [5]; these corrections have an angular asymmetry of  $\sim 2\%$  for muons and taus. Corrections due to higher orders in the  $Z^0$  exchange diagrams were *not* applied to the cross-sections; the resulting correction for the asymmetry will be discussed later. The errors shown in Figs. 1–4 are statistical; the additional normalisation uncertainties are indicated in Figs. 1b and 4, they are

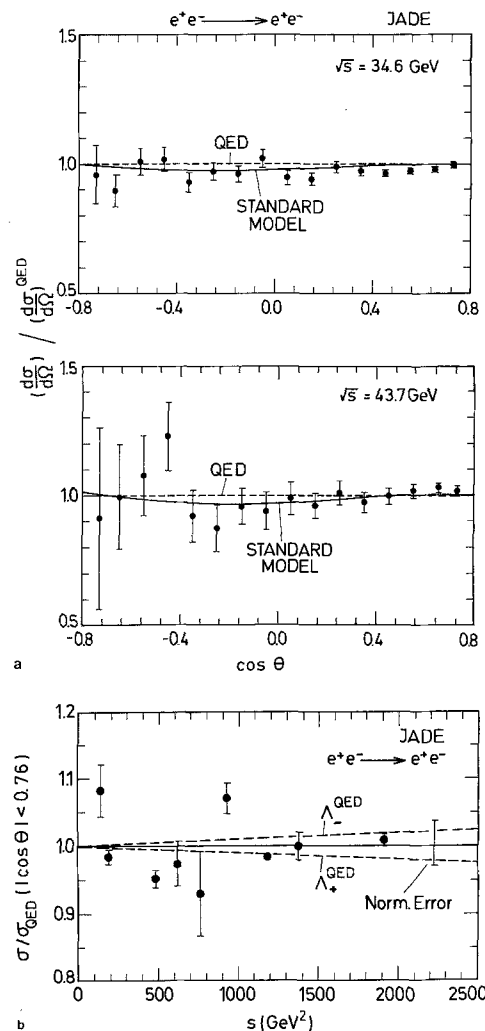


**Fig. 1.** **a** Angular distribution of  $e^+e^- \rightarrow e^+e^-$  at the two highest PETRA energies. The dashed lines are the QED predictions and the full lines the prediction by the standard model with  $\sin^2\theta_W = 0.217$ . **b** Ratio of the total cross-section for  $e^+e^- \rightarrow e^+e^-$  for  $|\cos \theta| < 0.76$  to the expectation from QED as a function of  $s$ . The error bars represent the statistical error; the normalisation uncertainty is indicated

3.2% for Bhabha scattering,  $\sim 5\%$  for muon pair production and  $\sim 4\%$  for tau pairs.

The luminosity was obtained from  $e^+e^- \rightarrow e^+e^-$  and  $e^+e^- \rightarrow \gamma\gamma$ . For the Bhabha cross-sections in Fig.1 the endcap region at polar angles of  $0.91 < |\cos\theta| < 0.955$  was used for normalisation, which has a systematic error of 2.8% and dominates the total normalisation error. For muon and tau-pairs the luminosity obtained in the barrel region,  $|\cos\theta| < 0.76$ , was used, which has a systematic error of 1.6% at  $\sqrt{s} \sim 34.5$  GeV and 2.5% at higher energies.

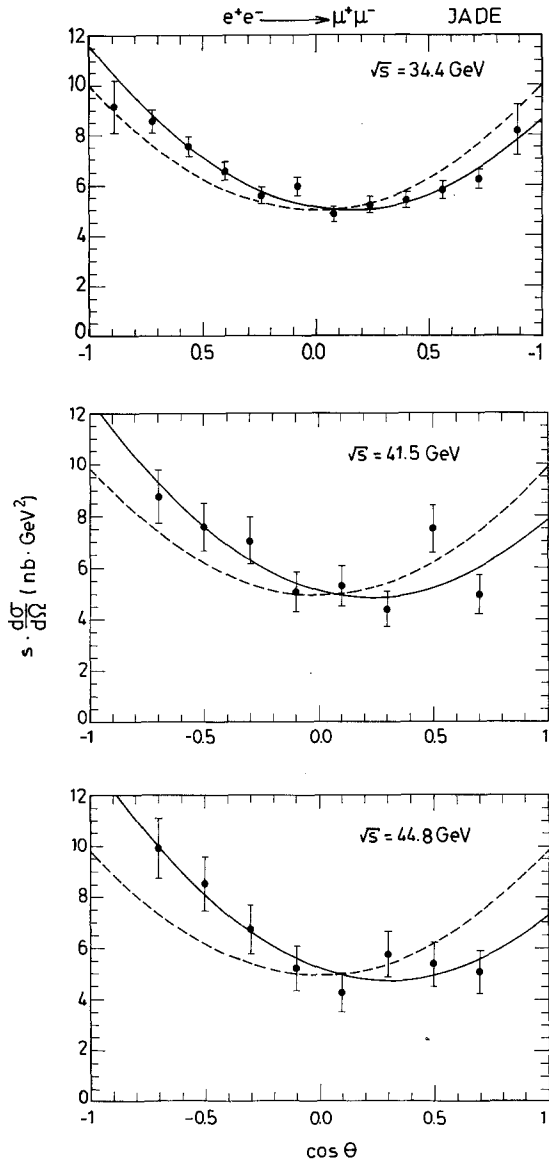


Fig. 2. Angular distribution of  $e^+e^- \rightarrow \mu^+\mu^-$  at the highest PETRA energies. The dashed lines are the symmetric QED predictions. The full lines are fits to the data allowing for an asymmetry

The angular distributions for  $e^+e^- \rightarrow e^+e^-$  are shown in Fig. 1a for the two highest PETRA energies relative to the expectation from QED; their shape agrees well with QED over the entire angular range. The total cross-section for  $|\cos\theta| < 0.76$  is shown as a function of  $s$  in Fig. 1b together with the

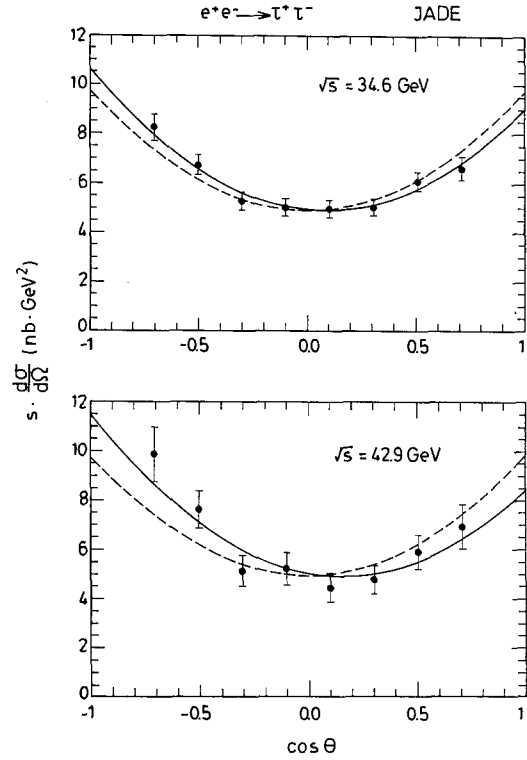


Fig. 3.  $e^+e^- \rightarrow \tau^+\tau^-$ . For explanations see Fig. 2

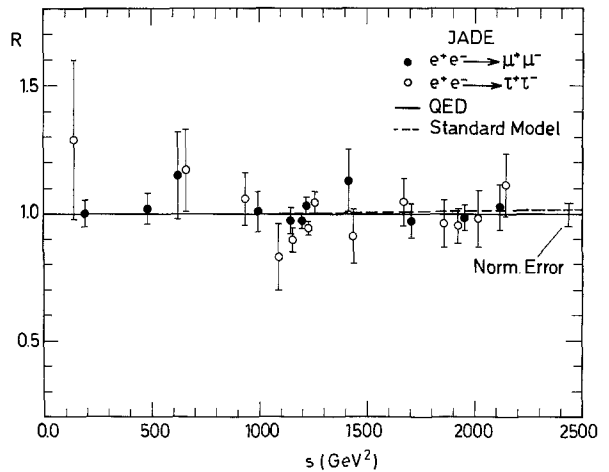


Fig. 4. The total cross-section ratio  $R = \frac{\sigma_{\mu\mu}}{\sigma_{\tau\tau}}$  as a function of  $s$  for muon and tau-pairs. The error bars correspond to the statistical error; the typical normalisation error is indicated. Compared to [4] the data points for muon pairs, which are close in  $s$  have been averaged for clarity

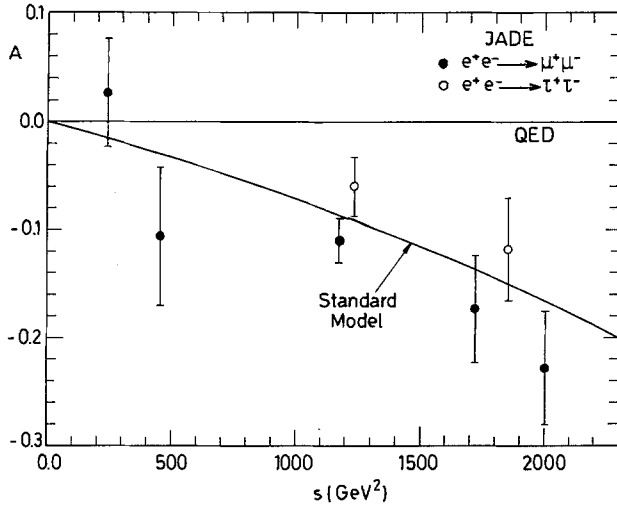


Fig. 5. The angular asymmetry for muons and taus as a function of  $s$ . The line labelled "standard model" was obtained using  $\chi_{II}$  with  $\sin^2\theta_w=0.217$  and  $M_Z=93$  GeV

QED expectation. Agreement within the errors is observed at all energies.

The shape of the angular distributions of muon (Fig. 2) and tau-pairs (Fig. 3) show a characteristic deviation from the prediction of pure QED (dashed lines) which is somewhat more pronounced for muons. Motivated by the electroweak cross-section which is given in the next section, the angular distributions are fit to a function  $1 + \cos^2\theta + \frac{8}{3}A \cos\theta$ . These fits are also shown in Figs. 2 and 3 (full lines). The asymmetry  $A$  is plotted in Fig. 5 as a function of  $s$  for muons and taus; it grows in absolute magnitude with increasing  $s$ .

Finally the ratio of the measured total cross-section for  $e^+e^- \rightarrow \mu^+\mu^-$  and  $\tau^+\tau^-$  to the QED expectation is shown in Fig. 4 at several values of  $s$ ; the agreement with QED is good for the entire  $s$ -range 144 GeV<sup>2</sup> to 2,000 GeV<sup>2</sup>.

### Electroweak Cross-Sections

Taking into account photon and  $Z^0$  exchange and including their interference, the differential cross-section for  $e^+e^- \rightarrow l^+l^-$  ( $l$  can be  $\mu$  or  $\tau$ ) is, in lowest order, given by [6]:

$$\frac{d\sigma}{d\Omega} = \frac{\alpha^2}{4s} (C_1(1 + \cos^2\theta) + C_2 \cos\theta) \quad (1)$$

where  $\theta$  is the polar angle of the fermion and

$$\begin{aligned} C_1 &= 1 + 2v_e v_l \chi + (v_e^2 + a_e^2)(v_l^2 + a_l^2) \chi^2 \\ C_2 &= -4a_e a_l \chi + 8v_e a_e a_l \chi^2 \end{aligned} \quad (2)$$

$v_e, v_l, a_e$  and  $a_l$  denote the vector and axial-vector weak couplings of electron and lepton  $l$  and  $\chi$  is a ratio of weak and electromagnetic constants, which will be discussed later. In the standard model the weak couplings, which are related to the weak isospin structure, are predicted to be  $a_l = -1$  and  $v_l = -1 + 4\sin^2\theta_w$ , where  $\theta_w$  is the weak mixing angle.

The integrated forward-backward or charge asymmetry introduced above is given by

$$A = \frac{3}{8} \frac{C_2}{C_1} \sim 1.5 \cdot a_e a_l \cdot \chi. \quad (3)$$

The approximation is valid at energies where the weak amplitude is small compared to the electromagnetic one; it is still good to a one percent accuracy even at the highest PETRA energy. The asymmetry is thus sensitive to the axial-vector weak coupling.

The total cross-section ratio

$$R = \frac{\sigma_{II}}{\sigma_0} = C_1 \quad \text{with} \quad \sigma_0 = \frac{4\pi\alpha^2}{3s} \quad (4)$$

will be used to deduce values for the vector coupling constants.

For  $\chi$  two parameterizations were used, namely:

$$\chi_I = \frac{\rho G_F M_Z^2}{8\pi\alpha\sqrt{2}} \frac{s}{s - M_Z^2}$$

and

$$\chi_{II} = \frac{1}{16\sin^2\theta_w \cos^2\theta_w} \frac{s}{s - M_Z^2}.$$

In parameterisation I of  $\chi$ ,  $e^+e^-$  annihilation is related to charged current processes, the free parameters are  $\alpha, G_F, M_Z$  and  $\rho$  in addition to the axial-vector and vector weak couplings  $a_l$  and  $v_l$ . The Fermi constant  $G_F$  and  $\alpha$  have been determined accurately [7] and their errors will be neglected ( $G_F = 1.166 \cdot 10^{-5}$  GeV<sup>-2</sup>). The mass  $M_Z$  of the  $Z^0$  was determined by the experiments at the  $p\bar{p}$  collider to be  $M_Z = 93 \pm 2$  GeV [8].  $\rho$  is defined as

$$\rho = \frac{M_W^2}{M_Z^2 \cos^2\theta_w}.$$

In the standard model at the Born level it is identical to 1, and we shall use this value when calculating coupling constants.

In parameterisation II, parameters from the neutral current sector are used, the free parameters besides  $a_l$  and  $v_l$  are  $\alpha, M_Z$  and  $\sin^2\theta_w$ .  $\sin^2\theta_w$  has been measured in many experiments in different reactions. We shall use the 1983 world average which

is dominated by data from deep inelastic neutrino scattering; including radiative corrections it is  $\sin^2\theta_w = 0.217 \pm 0.014$  [9]. In lowest order the two parameterisations of  $\chi$  are the same and are related by  $M_Z^2 = \pi\alpha/(\sqrt{2}G_F \sin^2\theta_w \cos^2\theta_w)$ .

Complete one-loop corrections have been calculated in both schemes [10, 11]. It turns out that a small correction has to be applied to the asymmetry when using  $\chi_I$  [10], while for parametrization II the one-loop corrections fortuitously cancel [11]. These additional corrections are therefore included in the theoretical prediction, which is then unique and is shown in Fig. 5 as a function of  $s$  and listed in Table 7 under  $A_{\text{St.M.}}$ . The asymmetry data for muons and taus follow closely the prediction of the standard model as can be seen in Fig. 5.

The cross-section for Bhabha scattering is slightly more complicated than (1) due to the contribution of the  $t$ -channel [6]:

$$\frac{d\sigma}{d\Omega} = \frac{\alpha^2}{8s} [4B_1 + (B_3 + B_2)(1 + \cos^2\theta) + 2(B_3 - B_2)\cos\theta] \quad (5)$$

where

$$B_1 = \left(\frac{s}{t}\right)^2 (1 + (v_e^2 - a_e^2)\chi')^2$$

$$B_2 = (1 + (v_e^2 - a_e^2)\chi)^2$$

$$2B_3 = \left(1 + \frac{s}{t} + (v_e + a_e)^2 \left(\frac{s}{t}\chi' + \chi\right)\right)^2$$

$$+ \left(1 + \frac{s}{t} + (v_e - a_e)^2 \left(\frac{s}{t}\chi' + \chi\right)\right)^2$$

and  $t = -0.5s(1 - \cos\theta)$  in the high energy limit.  $\chi$  was defined above and in order to obtain  $\chi'$ , the  $s$  in  $\chi$  has to be replaced by  $t$ . For Bhabha scattering the difference between using  $\chi_I$  and  $\chi_{II}$  is small compared to the experimental errors. The complete one-loop corrections have not yet been calculated but they have been estimated to be small and will therefore be neglected [13].

### Calculation of Coupling Constants

The simplest and most direct way to determine the axial-vector coupling constants for muons and taus is to calculate them by comparing (3) with the measured asymmetries. Averaging over all values of  $s$  and using  $M_Z = 93$  GeV yields:

$$a_e a_\mu = 1.30 \pm 0.17$$

$$a_e a_\tau = 0.74 \pm 0.22.$$

The errors include statistical and experimental systematic errors. The error due to the uncertainty of the  $Z$ -mass is negligible in comparison to the experimental errors.

The value for  $a_e a_\mu$  is nearly two standard deviations above and that for  $a_e a_\tau$  more than one standard deviation below the expectation. The  $\chi^2$  probability that the two values are equal is  $\sim 4\%$ .

The errors of the axial-vector coupling constants are dominated by the statistical uncertainties. The systematic errors, which have been discussed previously [4] are small for both, muons and taus, they are of the order  $\Delta A \lesssim 1\%$ . The systematic error of the muon pair asymmetry is dominated by the charge misidentification probability and apart from that it is difficult to imagine a background or detector effect that enlarges the asymmetry of the muons. The systematic error of the tau pair asymmetry, on the other hand, is dominated by the uncertainty of the background from Bhabha scattering, which has a large positive asymmetry. Careful analysis has however convinced us that the background has been properly taken into account. Radiative corrections come out to be essentially the same for both reactions, because they are calculated in the context of the standard model where universality is assumed. A deviation from the standard model might lead to a small difference.

At the present level of accuracy we consider the difference between the two axial-vector coupling constants to be due to a statistical fluctuation but hope to clarify this point with more data in the near future.

The axial-vector coupling constants have been determined in a similar way by CELLO, MARK J, PLUTO and TASSO at PETRA and by HRS, MAC and MARK II at PEP [12, 18, 24]. The average values of the PEP results and the averages of the PETRA results at medium and high energy are shown in Table 1 and compared to the JADE data\*.

**Table 1.** Axial-vector coupling constants from JADE and other  $e^+e^-$  experiments. For details see text

	$s$ (GeV <sup>2</sup> )	$a_e a_\mu$	$a_e a_\tau$
JADE	1,185	$1.27 \pm 0.24$	$0.68 \pm 0.30$
JADE	1,883	$1.32 \pm 0.24$	$0.78 \pm 0.31$
PEP	841	$0.99 \pm 0.12$	$0.88 \pm 0.16$
PETRA	1,190	$1.26 \pm 0.15$	$0.87 \pm 0.31$
PETRA	1,880	$1.09 \pm 0.16$	$0.87 \pm 0.25$

\* We have reevaluated the axial couplings from the asymmetry values given by the authors in order to avoid differences due to different values of  $M_Z$  or  $\sin^2\theta_w$ .

Most measurements at PEP and PETRA have the same tendency as our result:  $a_\tau$  is smaller than  $a_\mu$ , but the difference is not statistically significant.

The weak vector coupling constant can be calculated from (4). Assuming again  $M_Z=93$  GeV and setting  $a_e a_l=1$  one obtains, averaging over all energies:

$$v_e v_\mu = 0.04 \pm 0.31$$

$$v_e v_\tau = 0.31 \pm 0.27.$$

The quoted errors are statistical, a normalisation error of typically 4% leads to an error approximately three times the size of the statistical one. The results depend only weakly on the exact value of  $a_e a_l$ . The prediction of the standard model with  $\sin^2 \theta_W = 0.217$  is  $v_e v_l = 0.017$ , and both values agree well with it.  $v_\mu$  and  $v_\tau$  agree with each other within errors. The large errors of the vector coupling constants are characteristic for leptonic  $e^+ e^-$  reactions as the predicted deviation of the total cross-section from QED due to electroweak effects is only approximately 0.8% at  $s=2,000$  GeV<sup>2</sup>, well below the measurement errors.

For Bhabha scattering the prediction of the standard model with  $a_e = -1$  and  $v_e = -0.13$  is shown in Fig. 1a. The electroweak contributions only lead to a small deviation in the angular distribution with respect to QED. The expected difference is approximately 2% at  $\cos \theta \sim -0.2$  for  $s=1,195.0$  GeV<sup>2</sup> and 4.4% for  $s=1,910.4$  GeV<sup>2</sup>. The experimental errors are of the same order of magnitude at the lower  $s$  value and twice as large for the higher value of  $s$ . Under the assumption that the weak neutral current is described by the standard model the weak coupling constants for electrons were deduced in a combined fit of  $a_e$  and  $v_e$ . They are shown in line 1 of Table 2 and come out close to the expectation.

The experimental results for the axial-vector and vector coupling constants of electrons, muons and taus are consistent with universality. So one can assume universality to obtain more accuracy. The separate results of two dimensional fits of  $a_l$  and  $v_l$  for the muon and tau data, where  $e-\mu^-$  and  $e-\tau^-$

universality were assumed respectively, are shown in lines 2 and 3 of Table 2. Finally a common fit was made to all data; the results are shown in the last line of Table 2. The prediction of the standard model for the axial-vector coupling constant is confirmed with a reduced error of 10%.

The weak coupling constants have been determined also in neutrino scattering off electrons, which is also a purely leptonic process. There, two sets of solutions exist, one of which is excluded by the  $e^+ e^-$  measurements. The remaining solution is [14]:

$$a_e = 2g_A = -0.990 \pm 0.052$$

$$v_e = 2g_V = -0.076 \pm 0.094$$

in good agreement with the  $e^+ e^-$  values.

### Determination of $\rho$ , $\sin^2 \theta_W$ and $M_Z$

A different aspect of the standard model is tested by determining the parameter  $\rho$  in  $\chi_1$ . It appears in  $\chi_1$  because the charged current coupling constant  $G_F$  is used for a neutral current process. Its size is determined by the Higgs structure of the model and it is 1 in models with Higgs doublets, as e.g. the standard model.  $\rho$  and the axial-vector coupling constants are strongly correlated. When determining  $\rho$  the predictions of the standard model for  $a$  and  $v$  were assumed. Then one obtains:

$$\rho = 1.32 \pm 0.16 \quad \text{for } \mu\mu$$

$$\rho = 1.09 \pm 0.12 \quad \text{for } ee, \mu\mu, \tau\tau.$$

The dependence on the mass of the  $Z$  is weak, typically  $\Delta\rho=0.01$  for  $\Delta M_Z=2$  GeV. The numerical result is very similar to that of the axial-vector couplings. It agrees with the expectation of 1 and with measurements at the  $p\bar{p}$ -collider [8] and in neutrino scattering [14, 15].

The data can be interpreted in yet another way: Using parameterization II of  $\chi$ , constraints can be obtained on  $\sin^2 \theta_W$  and  $M_Z$ . Here again we use the predictions of the standard model for  $a$  and  $v$ . The contours at 95% confidence level in the  $\sin^2 \theta_W, M_Z$  plane are shown in Fig. 6 for  $\mu$ -pairs alone and for the combined data of  $\mu^+ \mu^-$  and  $\tau^+ \tau^-$ . The contour follows the prediction of the standard model, its width is related to the errors of the angular asymmetry and the "length" depends strongly on the normalisation factor [16]. Due to the shape of this contour a simultaneous precise determination of  $\sin^2 \theta_W$  and  $M_Z$  are not possible. Fixing one of the two parameters leads to the following results for a

**Table 2.** Coupling constants from 2-parameter fits and results for  $\sin^2 \theta_W$

Input	$ a_l $	$ v_l $	$\sin^2 \theta_W$
$e^+ e^-$	$0.96^{+0.28}_{-0.53}$	$0.30 \pm 0.33$	$0.26 \pm 0.10$
$\mu^+ \mu^-$	$1.16 \pm 0.12$	$0.33 \pm 0.33$	$0.15 \pm 0.02$
$\tau^+ \tau^-$	$0.88^{+0.18}_{-0.21}$	$0.53^{+0.18}_{-0.28}$	—
$e^+ e^-, \mu^+ \mu^-, \tau^+ \tau^-$	$1.04 \pm 0.10$	$0.36 \pm 0.28$	$0.18^{+0.03}_{-0.02}$

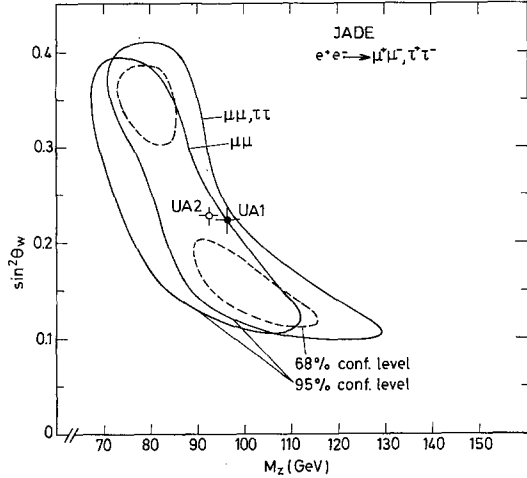


**Fig. 6.** 95% and 68% confidence level contours in the  $(\sin^2 \theta_w, M_Z)$  plane from  $e^+e^- \rightarrow \mu^+\mu^-$  and  $\tau^+\tau^-$  in comparison with the measured points from UA1 and UA2 at the  $p\bar{p}$ -collider

combined analysis of muons and taus:

$$\sin^2 \theta_w = 0.17^{+0.03}_{-0.02} \pm 0.01 \quad \text{with} \\ M_Z = (93 \pm 2) \text{ GeV fixed.}$$

The second error is due to the uncertainty in  $M_Z$ . The result changes only slightly when also the Bhabha data are included (Table 2). It agrees with the radiatively corrected world average of  $0.217 \pm 0.014$  [9] and with values obtained by other PETRA experiments [17, 18].

Using  $\sin^2 \theta_w = 0.217$  as input one determines the mass of the  $Z$  to be:

$$M_Z = (91 \pm 5) \text{ GeV} \quad \text{for } \mu\mu, \tau\tau.$$

Muon data alone gives  $84 \pm 5$  GeV.

### Limits on Deviations from the Standard Model

As has been demonstrated in the previous sections, the measured cross-sections are consistent with the standard model within the experimental accuracy. In the following we investigate the deviations from the standard model allowed by the data. We put limits on a possible deviation from the point-like nature of leptons, on the mass-scale of possible sub-constituents and investigate the consequences of the existence of another gauge group in addition to the standard  $SU(2) \times U(1)$ . The theoretical background for these limits has been discussed extensively in the literature [19–23] and we shall therefore be brief.

Deviations from the point-like nature of leptons are usually parameterised by introducing in the QED cross-sections form-factors of the form:

**Table 3.** Cut-off parameters: Lower limits at 95% confidence level

	QED		COMP. MODELS					
			LL, RR		AA		VV	
	$A_+^{\text{QED}}$	$A_-^{\text{QED}}$	$A_+^{\text{comp}}$	$A_-^{\text{comp}}$	$A_+^{\text{comp}}$	$A_-^{\text{comp}}$	$A_+^{\text{comp}}$	$A_-^{\text{comp}}$
	(GeV)		(TeV)		(TeV)		(TeV)	
$e^+e^-$	267	200	1.1	1.4	2.4	2.3	2.5	3.1
$\mu^+\mu^-$	230	245	4.4	2.1	7.5	2.8	5.8	4.8
$\tau^+\tau^-$	285	210	2.2	3.2	2.7	5.7	4.1	5.7

$$F(q^2) = 1 \mp \frac{q^2}{q^2 - (A_{\pm}^{\text{QED}})^2}$$

$A^{\text{QED}}$  is the QED cut-off parameter. In Bhabha scattering form-factors are added in the  $s$ - and the  $t$ -channel, but it is assumed that they have the same cut-off parameter; the form-factors lead to a modification of the angular distribution. The lower limits obtained from the data at 95% confidence are given in Table 3.

For  $e^+e^- \rightarrow \mu^+\mu^-$  and  $\tau^+\tau^-$  only the total rate is modified by the introduction of a form-factor. The 95% confidence lower limits obtained by comparing to the measured total cross-sections are also listed in Table 3.

All cut-off parameters are larger than 200 GeV up to the highest values of  $s$  around 2,000 GeV<sup>2</sup>.

A more detailed test of a substructure of quarks and leptons has been proposed by Eichten et al. [20, 21]. They assume that the standard model is correct at low energies but add to the photon and  $Z^0$  exchange contact interactions, which lead to the following effective Lagrangian which has to be added to the standard one:

$$L_{\text{eff}} = \frac{g^2}{2A_{\pm}^{\text{comp}}} \cdot [\eta_{LL} j_L j_L + \eta_{RR} j_R j_R + 2\eta_{RL} j_R j_L].$$

The parameter  $A^{\text{comp}}$  gives the compositeness mass scale. It is defined such that the coupling constant  $\frac{g^2}{4\pi} = 1$ . The sign in the subscript of  $A^{\text{comp}}$  indicates the overall sign of the addition to the standard cross-section. The additional interaction does not necessarily conserve parity, therefore the left- and right-handed currents  $j_L$  and  $j_R$  appear separately. Depending on the type of modification expected the  $\eta$ 's assume values of 0 or  $\pm 1$ . Pure left-handed ( $\eta_{LL} = 1$ , the others 0) and pure right-handed interactions ( $\eta_{RR} = 1$ , the others 0) lead to the same modification and are thus indistinguishable. For axial-vector interactions (AA)  $\eta_{LL} = \eta_{RR} = +1$  and  $\eta_{RL} = -1$  and for vector (VV)  $\eta_{LL} = \eta_{RR} = \eta_{RL} = 1$ .

**Table 4.** Measured differential cross-sections for  $e^+e^- \rightarrow e^+e^-$ 

$\cos\theta$	$s = 1,195.0 \text{ GeV}^2$		$s = 1,910.4 \text{ GeV}^2$	
	$\frac{d\sigma}{d\Omega}$ (pb)	$\frac{d\sigma}{d\Omega} / \left(\frac{d\sigma}{d\Omega}\right)_{\text{QED}}$	$\frac{d\sigma}{d\Omega}$ (pb)	$\frac{d\sigma}{d\Omega} / \left(\frac{d\sigma}{d\Omega}\right)_{\text{QED}}$
-0.73	$17.38 \pm 2.03$	$0.961 \pm 0.112$	$10.34 \pm 3.95$	$0.914 \pm 0.349$
-0.65	$16.77 \pm 1.15$	$0.898 \pm 0.062$	$11.61 \pm 2.34$	$0.995 \pm 0.201$
-0.55	$19.91 \pm 0.97$	$1.011 \pm 0.049$	$13.28 \pm 1.89$	$1.078 \pm 0.153$
-0.45	$21.59 \pm 0.94$	$1.020 \pm 0.044$	$16.29 \pm 1.75$	$1.230 \pm 0.132$
-0.35	$21.66 \pm 0.84$	$0.932 \pm 0.036$	$13.37 \pm 1.46$	$0.920 \pm 0.100$
-0.25	$25.36 \pm 0.86$	$0.973 \pm 0.033$	$14.25 \pm 1.40$	$0.874 \pm 0.086$
-0.15	$28.92 \pm 0.87$	$0.964 \pm 0.029$	$17.97 \pm 1.28$	$0.957 \pm 0.068$
-0.05	$36.42 \pm 1.04$	$1.025 \pm 0.029$	$20.88 \pm 1.55$	$0.939 \pm 0.070$
0.05	$41.32 \pm 1.10$	$0.951 \pm 0.025$	$26.92 \pm 1.69$	$0.990 \pm 0.062$
0.15	$51.92 \pm 1.14$	$0.944 \pm 0.021$	$33.09 \pm 1.60$	$0.961 \pm 0.047$
0.25	$72.16 \pm 1.35$	$0.992 \pm 0.019$	$46.07 \pm 2.06$	$1.012 \pm 0.045$
0.35	$98.40 \pm 1.58$	$0.975 \pm 0.016$	$61.69 \pm 2.31$	$0.977 \pm 0.037$
0.45	$143.91 \pm 1.97$	$0.967 \pm 0.013$	$93.17 \pm 2.92$	$1.000 \pm 0.031$
0.55	$232.35 \pm 2.43$	$0.976 \pm 0.010$	$152.27 \pm 3.59$	$1.023 \pm 0.024$
0.65	$420.38 \pm 3.30$	$0.982 \pm 0.008$	$276.95 \pm 4.89$	$1.034 \pm 0.018$
0.73	$756.72 \pm 6.16$	$1.000 \pm 0.008$	$483.86 \pm 8.77$	$1.022 \pm 0.019$

**Table 5.** Measured differential cross-sections for  $e^+e^- \rightarrow \mu^+\mu^-$  and  $\tau^+\tau^-$ 

$e^+e^- \rightarrow \mu^+\mu^-$			$e^+e^- \rightarrow \tau^+\tau^-$			
$s = 1,181.7 \text{ GeV}^2$		$s = 1,721.7 \text{ GeV}^2$	$s = 2,004.1 \text{ GeV}^2$		$s = 1,195.0 \text{ GeV}^2$	$s = 1,853.3 \text{ GeV}^2$
$\cos\theta$	$s \frac{d\sigma}{d\Omega}$ (nb GeV <sup>2</sup> )	$\cos\theta$	$s \frac{d\sigma}{d\Omega}$ (nb GeV <sup>2</sup> )	$s \frac{d\sigma}{d\Omega}$ (nb GeV <sup>2</sup> )	$s \frac{d\sigma}{d\Omega}$ (nb GeV <sup>2</sup> )	$s \frac{d\sigma}{d\Omega}$ (nb GeV <sup>2</sup> )
-0.89	$9.17 \pm 1.05$					
-0.72	$8.58 \pm 0.44$					
-0.56	$7.56 \pm 0.38$	-0.7	$8.76 \pm 1.03$	$9.90 \pm 1.18$	$8.28 \pm 0.54$	$9.87 \pm 1.11$
-0.40	$6.56 \pm 0.35$	-0.5	$7.58 \pm 0.93$	$8.50 \pm 1.06$	$6.77 \pm 0.39$	$7.61 \pm 0.77$
-0.24	$5.60 \pm 0.32$	-0.3	$7.02 \pm 0.89$	$6.70 \pm 0.94$	$5.31 \pm 0.34$	$5.12 \pm 0.62$
-0.08	$5.94 \pm 0.34$	-0.1	$5.05 \pm 0.75$	$5.17 \pm 0.83$	$5.06 \pm 0.33$	$5.20 \pm 0.63$
0.08	$4.86 \pm 0.30$	0.1	$5.27 \pm 0.76$	$4.23 \pm 0.75$	$5.01 \pm 0.33$	$4.43 \pm 0.58$
0.24	$5.21 \pm 0.31$	0.3	$4.38 \pm 0.68$	$5.73 \pm 0.86$	$5.06 \pm 0.33$	$4.76 \pm 0.56$
0.40	$5.39 \pm 0.31$	0.5	$7.51 \pm 0.90$	$5.37 \pm 0.83$	$6.14 \pm 0.36$	$5.88 \pm 0.66$
0.56	$5.80 \pm 0.32$	0.7	$4.98 \pm 0.74$	$5.06 \pm 0.81$	$6.66 \pm 0.46$	$6.89 \pm 0.88$
0.72	$6.24 \pm 0.35$					
0.89	$8.19 \pm 1.00$					

**Table 6.** Total cross-sections for  $e^+e^- \rightarrow \mu^+\mu^-$  and  $\tau^+\tau^-$ 

$e^+e^- \rightarrow \mu^+\mu^-$		$e^+e^- \rightarrow \tau^+\tau^-$	
$s$ (GeV <sup>2</sup> )	$R = \sigma/\sigma_0$	$s$ (GeV <sup>2</sup> )	$R = \sigma/\sigma_0$
192.4	$1.00 \pm 0.05$	144.0	$1.29 \pm 0.24$
484.0	$1.02 \pm 0.06$	655.4	$1.16 \pm 0.16$
628.0	$1.15 \pm 0.17$	936.4	$1.06 \pm 0.10$
995.3	$1.01 \pm 0.08$	1,087.7	$0.83 \pm 0.13$
1,145.1	$0.97 \pm 0.05$	1,154.6	$0.90 \pm 0.05$
1,197.9	$0.97 \pm 0.02$	1,197.2	$0.94 \pm 0.03$
1,217.3	$1.03 \pm 0.03$	1,225.0	$1.04 \pm 0.04$
1,413.8	$1.12 \pm 0.12$	1,427.3	$0.91 \pm 0.11$
1,704.4	$0.97 \pm 0.06$	1,669.5	$1.05 \pm 0.09$
1,950.6	$0.98 \pm 0.05$	1,855.9	$0.96 \pm 0.09$
2,115.8	$1.03 \pm 0.09$	1,951.9	$0.95 \pm 0.07$
		2,014.2	$0.98 \pm 0.11$
		2,140.0	$1.11 \pm 0.12$

The 95% confidence lower limits on  $\Lambda^{\text{comp}}$  are listed in Table 3. They are of the order of several TeV. For  $e^+e^- \rightarrow \mu^+\mu^-$  and  $\tau^+\tau^-$  the limits are only valid for the case that there are common sub-constituents in the initial and final state.

A further modifications of the standard model proposed some time ago is the addition of another group  $G$  to the standard  $SU(2) \times U(1)$  [22, 23].  $G$  can be another  $U(1)$  or  $SU(2)$  and implies the existence of a second neutral gauge boson in addition to the  $Z^0$ . The addition of  $G$  leads to a modification of the vector coupling constant

$$v^2 = (-1 + 4 \sin^2 \theta_w)^2 \rightarrow v^2 = (-1 + 4 \sin^2 \theta_w)^2 + 16 C.$$

Therefore no modification of the angular asymmetry for muon and tau pairs is expected. The 95% con-



**Table 7.** Asymmetries for  $e^+e^- \rightarrow \mu^+\mu^-$  and  $\tau^+\tau^-$ 

$s(\text{GeV}^2)$	$\int Ldt(\text{pb}^{-1})$	Events	$A(\%)$	$A_{\text{St.M.}}(\%)$
$e^+e^- \rightarrow \mu^+\mu^-$				
192.0	1.6	458	+ 2.7±4.9	- 1.2
484.0	2.4	264	-10.6±6.4	- 3.2
1,181.7	71.2	3,400	-11.1±1.8±1.0	- 8.6
1,721.7	13.2	461	-17.3±4.8±1.0	-13.7
2,004.1	13.4	372	-22.8±5.1±1.0	-16.6
$e^+e^- \rightarrow \tau^+\tau^-$				
1,195.0	62.4	1,998	- 6.0±2.5±1.0	- 8.8
1,853.3	26.6	575	-11.8±4.6±1.0	-14.9

confidence upper limit on  $C$  from muon and tau pairs is  $C < 0.04$  and from Bhabha scattering  $C < 0.030$ .

Similar limits have been obtained by the other experiments at PETRA and PEP [18, 24].

## Summary

The cross-sections for  $e^+e^- \rightarrow e^+e^-$ ,  $\mu^+\mu^-$  and  $\tau^+\tau^-$  were measured with the JADE detector at center-of-mass energies of  $12 \leq \sqrt{s} \leq 46.78$  GeV. The data which were obtained between 1980 and 1984 and have partially been published before, are compared to predictions of the standard model.

The differential and total cross-sections for Bhabha scattering and the total cross-sections for muon- and tau-pair production were found to agree with QED, the lower limits on the QED cut-off parameters were determined to be larger than 200 GeV.

The differential cross-sections for muon- and tau-pairs show a forward-backward asymmetry which excludes the validity of pure QED. The values of the asymmetry and their  $s$ -dependance is compatible with the prediction of the standard model using  $M_Z = 93$  GeV. The axial-vector and vector coupling constants were determined, they are compatible with universality although a small difference between  $a_\mu$  and  $a_\tau$  is not excluded. From a global fit assuming universality we get  $|a_1| = 1.04 \pm 0.10$  and  $|v_1| = 0.36 \pm 0.28$ .

Assuming the standard values of  $a_1$  and  $v_1$ , constraints on  $\sin^2\theta_W$  and  $M_Z$  were obtained; fixing  $\sin^2\theta_W = 0.217$  yields  $M_Z = (91 \pm 5)$  GeV for the combined set of muons and tau data; a result well compatible with the UA1 and UA2 measurements. Using  $M_Z = 93$  GeV one obtains  $\sin^2\theta_W = 0.18_{-0.02}^{+0.03} \pm 0.01$ , a value which is within one standard deviation of recent measurements in other reactions. The  $\rho$ -parameter was determined to be  $1.09 \pm 0.12$  using the data from all three reactions and assuming  $M_Z = 93$  GeV.

The data have also been used to obtain limits on deviations from the standard model. For the composite scale parameters a la Eichten et al. values of 1–6 TeV are obtained depending on the chirality of the new interaction. If an additional gauge group were present which leads to an additional term of  $16C$  in the square of the vector coupling constant, the 95% confidence lower limit on  $C$  is found to be  $C < 0.030$ .

*Acknowledgements.* We are indebted to the PETRA machine group and the DESY computer center staff for their excellent support during the experiment and to all the engineers and technicians of the collaborating institutions who have participated in the construction and maintenance of the apparatus. This experiment was supported by the Bundesministerium für Forschung und Technologie, by the Japanese Ministry of Education, Science and Culture, by the UK Science and Engineering Research Council through the Rutherford Appleton Laboratory and by the US Department of Energy. The visiting groups at DESY wish to thank the DESY directorate for the hospitality extended to them.

## References

1. S.L. Glashow: Nucl. Phys. **22**, 579 (1961); Rev. Mod. Phys. **52**, 539 (1980); A. Salam: Phys. Rev. **127**, 331 (1962); Rev. Mod. Phys. **52**, 525 (1980); S. Weinberg: Phys. Rev. Lett. **19**, 1264 (1967); Rev. Mod. Phys. **52**, 515 (1980)
2. JADE Collab. W. Bartel et al.: Phys. Lett. **88B**, 171 (1979); Phys. Lett. **92B**, 206 (1980)
3. H. Drumm et al. in: Wire Chamber Conf. pp. 333, eds. W. Bartel, M. Regler. Amsterdam: North Holland 1980; J. Allison et al.: Nucl. Instrum. Methods **A238**, 220 (1985); Nucl. Instrum. Methods **A238**, 230 (1985)
4. JADE Collab. W. Bartel et al.: Z. Phys. C – Particles and Fields **26**, 507 (1985); JADE Collab. W. Bartel et al.: Z. Phys. C – Particles and Fields **19**, 197 (1983); JADE Collab. W. Bartel et al.: Phys. Lett. **161B**, 188 (1985)
5. F.A. Berends, R. Kleiss, S. Jadach: Nucl. Phys. **B202**, 63 (1982); F.A. Berends et al.: Nucl. Phys. **57B**, 381 (1973); Nucl. Phys. **61B**, 414 (1973); Nucl. Phys. **63B**, 381 (1973); Nucl. Phys. **68B**, 541 (1974); Nucl. Phys. **177B**, 237 (1981); Phys. Lett. **63B**, 432 (1976)
6. R. Budny: Phys. Lett. **45B**, 340 (1973); Phys. Lett. **55B**, 227 (1975)
7. Particle Data Book: Rev. Mod. Phys. **52** (1980)
8. UA1 Collab. G. Arnison et al.: Phys. Lett. **126B**, 398 (1983); Phys. Lett. **129B**, 273 (1983); UA2 Collab. P. Bagnaia et al.: Z. Phys. C – Particles and Fields **24**, 1 (1984)
9. A. Sirlin, W.J. Marciano: Nucl. Phys. **B189**, 442 (1981); W.J. Marciano: 1983 Int. Symposium on Lepton and Photon Interactions at High Energies, pp. 80. Eds. D.G. Cassel, D.L. Kreinick, Cornell University, 1983
10. W. Wetzel: Nucl. Phys. **B227**, 1 (1983); Preprint Heidelberg (1983). At  $s=1,195$  GeV<sup>2</sup>  $\Delta A = +0.6\%$  and at  $s=1,853$  GeV<sup>2</sup>  $\Delta A = +1.1\%$  were used
11. M. Boehm, W. Hollik: Nucl. Phys. **B204**, 45 (1982); Z. Phys. C – Particles and Fields **23**, 31 (1984); R.W. Brown, K. Decker, E.A. Paschos: Phys. Rev. Lett. **52**, 1192 (1984)
12. A summary of recent (partially unpublished) results can be

- found in: B. Naroska: Physics in Collisions V. Autun, France, Eds. B. Aubert, L. Montanet, p. 287 (1985); CELLO Collab. H.J. Behrend et al.: Z. Phys. C – Particles and Fields **14**, 283 (1983); Phys. Lett. **114B**, 282 (1982); HRS Collab. M. Derrick et al.: Phys. Rev. **D31**, 2352 (1985); HRS Collab. K.K. Gan et al.: Phys. Lett. **153B**, 116 (1985); MARKJ Collab. B. Adeva et al.: Phys. Rev. Lett. **55**, 665 (1985); MARKII Collab. N.E. Levi et al.: Phys. Rev. Lett. **51**, 1941 (1983); PLUTO Collab. Ch. Berger et al.: Z. Phys. C – Particles and Fields **28**, 1 (1985); TASSO Collab. M. Althoff et al.: Z. Phys. C – Particles and Fields **26**, 521 (1985)
13. M. Boehm et al.: Phys. Lett. **144B**, 414 (1984)
  14. W. Krenz: Aachen preprint PITHA 84/42 (1984); submitted to Nucl. Phys. B
  15. CHARM Collab. F. Bergsma et al.: Phys. Lett. **147B**, 481 (1984); L.A. Ahrens et al.: Phys. Rev. Lett. **54**, 18 (1984)
  16. D.H. Saxon: Physics in Collisions IV. Ed. A. Seiden, UC Santa Cruz
  17. A. Boehm: Measurement of  $\sin^2\theta_W$  from the reaction  $e^+e^- \rightarrow \mu^+\mu^-$ , Un. Aachen Preprint PITHA 84/11 (1984); MARKJ Collab. B. Adeva et al.: Phys. Rev. Lett. **54**, 665 (1985)
  18. PLUTO Collab. Ch. Berger et al.: Z. Phys. C – Particles and Fields **27**, 341 (1985)
  19. S.D. Drell: Ann. Phys. **75**, 4 (1958)
  20. M.E. Peskin: Proc. Int. Symp. on Lepton and Photon Interactions at High Energies (1981), ed. W. Pfeil. Phys. Inst. der Universität Bonn
  21. E.J. Eichten, K.D. Lane, M.E. Peskin: Phys. Rev. Lett. **50**, 811 (1983)
  22. E.H. de Groot, G.J. Gounaris, D. Schildknecht: Phys. Lett. **85B**, 399 (1979); Phys. Lett. **90B**, 427 (1980); Z. Phys. C – Particles and Fields **5**, 127 (1980); Phys. Lett. **95B**, 128 (1980)
  23. M. Kuroda, D. Schildknecht, K.-H. Schwarzer: Bielefeld preprint BI-TP 84/22 (1984)
  24. CELLO Collab. H.J. Behrend et al.: Z. Phys. C – Particles and Fields **14**, 283 (1983); MARKJ Collab. B. Adeva et al.: Phys. Rep. **109**, 133 (1984); TASSO Collab. M. Althoff et al.: Z. Phys. C – Particles and Fields **22**, 13 (1984); HRS Collab. D. Bender et al.: Phys. Rev. **D30**, 515 (1984)